JACS Au
AN OPEN ACCESS JOURNAL OF THE AMERICAN CHEMICAL SOCIETY

pubs.acs.org/jacsau
Article

Early-Onset Parkinson Mutation Remodels Monomer−Fibril Interactions to Allosterically Amplify Synuclein's Amyloid Cascade

Jinfeng Huang, Rashik Ahmed, Madoka Akimoto, Karla Martinez Pomier, and Giuseppe Melacini*

Cite This: JACS Au 2023, 3, 3485−3493
Read Online

ACCESS | Metrics & More | Article Recommendations | Supporting Information

ABSTRACT: Alpha synuclein (αS) aggregates are the main component of Lewy bodies (LBs) associated with Parkinson's disease (PD). A longstanding question about αS and PD pertains to the autosomal dominant E46K αS mutant, which leads to the early onset of PD and LB dementias. The E46K mutation not only promotes αS aggregation but also stabilizes αS monomers in "closed" conformers, which are compact and aggregation-incompetent. Hence, the mechanism of action of the E46K mutation is currently unclear. Here, we show that αS monomers harboring the E46K mutation exhibit more extensive interactions with fibrils compared to those of WT. Such monomer-fibril interactions are sufficient to allosterically drive transitions of αS monomers from closed to open conformations, enabling αS aggregation. We also show that E46K promotes head-to-tail monomer−monomer interactions in early self-association events. This multipronged mechanism provides a new framework to explain how the E46K mutation and possibly other αS variants trigger early-onset PD.

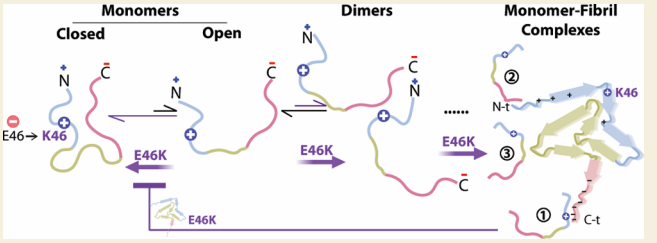

KEYWORDS: *alpha synuclein, inherited mutation, nuclear magnetic resonance; allostery, monomer−fibril interactions*

INTRODUCTION

Parkinson's disease (PD) is a progressive neurodegenerative disorder associated with cognitive decline and motor deficit.[1−4] A clinical hallmark of PD is the presence of insoluble inclusions *i.e.*, Lewy bodies (LBs).[1−6] The main component of LBs is alpha synuclein (αS, Figure 1A) in its aggregated forms, which contribute to cellular toxicity.[1,7] The central role of αS aggregation in PD pathogenesis is confirmed by the observation that several inherited αS mutations leading to early PD-onset also increase the aggregation propensity of αS.[8−13] However, only limited understanding is currently available about the mechanisms underlying how familial αS mutations alter the aggregation of monomeric αS into fibrils.

In its monomeric form, αS is an intrinsically disordered protein (IDP) that samples a wide range of dynamic conformations, including both "closed" and "open" states (Figure 1B).[14−22] Closed conformers are stabilized by electrostatic interactions between the positively and negatively charged αS N- and C-termini (NTR and CTR), respectively, which occlude the aggregation-prone and fibrillization-essential non-amyloid-β component (NAC) region (Figure 1A, B). In the open conformers, the NAC segment is exposed and available to self-associate into oligomers and fibrils (Figure 1A, B).[14,15,23] Once formed, wild-type (wt) αS fibrils recruit additional monomers primarily through electrostatic interactions between the fibril C-terminus and the monomer N-terminus, driving closed-to-open monomer transitions and promoting secondary nucleation and further elongation of αS fibrils.[24−31] Understanding how PD-related mutations alter these self-association equilibria from monomer to fibrils (Figure 1B) is essential to understanding the molecular etiology of PD and possibly other amyloid-driven dementias.[32−34]

Among known αS mutations causing early-onset PD, the autosomal dominant E46K has garnered significant interest due to its implications not only for PD specifically but also for LB dementias (LBDs) in general.[35,36] Yet, several open questions remain about how E46K affects αS to trigger PD. The +2 charge change introduced by the E46K mutation strengthens the electrostatic attraction between the N- and C-termini of monomeric αS stabilizing the closed conformers (Figure 1B), as confirmed by an elution delay in size exclusion chromatography (Figure 1C), ^{15}N-R_2 measurements (Figure S1) and by previous molecular dynamics (MD) simulations and paramagnetic relaxation enhancements (PREs).[37,38] The E46K-induced stabilization of closed αS monomers with a shielded NAC region is expected to delay αS aggregation (Figure 1B). However, ThT fluorescence data (Figure 1D) show that the E46K mutation unexpectedly elicits the opposite

Received: October 26, 2023
Revised: November 13, 2023
Accepted: November 14, 2023
Published: December 13, 2023

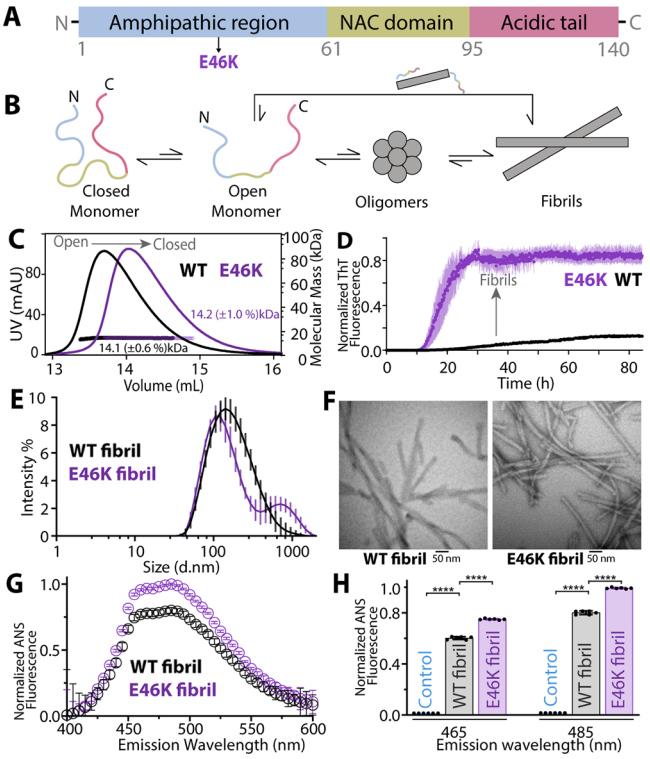

Figure 1. (A) Domain architecture of αS and location of the PD-related early onset mutation E46K. The net charges of the N-, NAC and C-terminal regions of αS are +4 for wt (+6 for E46K), −1 and −12, respectively. (B) Mechanism of αS fibril formation. 'Closed' monomer conformers are stabilized by electrostatic interactions between the N- and C-terminal regions, which shield the NAC region. In "open" monomers, the NAC region is available for self-association into primary nuclei, oligomers, and eventually fibrils. The latter recruit monomers to further accelerate fibril elongation and secondary nucleation. (C) SEC-MALS measurements for αS monomers. Size exclusion chromatography profiles and molecular weights are shown for wt and E46K αS monomers. E46K enhances the electrostatic attraction between the N- and C-terminal regions of αS, resulting in a more compact ensemble. (D) Time-dependent Thioflavin T (ThT) fluorescence for wt and E46K αS, showing that E46K amplifies αS aggregation. (E) DLS measurements of wt and E46K αS fibrils after ultracentrifugation. (F) TEM images of preformed αS fibrils after ultracentrifugation. (G) Fluorescence of ANS bound to 250 μM wt and E46K fibrils. (H) Fluorescence of ANS at emission wavelengths of 465 and 485 nm. Two-way ANOVA was used to determine the statistical significance for the wt *vs* E46K comparisons with **** representing p-values <0.0001.

effect. The E46K mutation not only accelerates αS aggregation by shortening the lag time but also increases the ThT fluorescence at the plateau (Figure 1D). These ThT-based results are in agreement with our dynamic light scattering (DLS) and negative stain transmission electron microscopy (TEM) data (Figures 1E, F and S2), with the enhanced β-sheet formation observed by circular dichroism[11,12,39,40] for the E46K mutant compared to wt αS, and with the increased αS aggregation propensity revealed by cross-linking-based sodium dodecyl sulfate polyacrylamide gel electrophoresis,[40,41] as well as with Western blot and EM analyses of cultured cells.[9,10,42] Nevertheless, it is not fully understood how the amplification of αS aggregation can be reconciled with the E46K-induced shift to aggregation-averse closed αS monomers.

Existing hypotheses for the enhanced aggregation of E46K αS are primarily based on fibril structures.[36,43−46] Solid-state NMR and cryo-EM consistently point to structural differences in E46K *vs* wt αS fibrils reflecting rewired electrostatic networks.[36,43,44,47,48] The mutation from glutamic acid to lysine at position 46 breaks the intrafilament E46-K80 salt bridge and introduces new intra- and inter-filament salt bridges, resulting in fibrils ∼14 kcal/mol/layer more stable than wt αS.[36] Besides the introduction of a series of novel electrostatic interactions between fibril filaments, the E46K mutation also perturbs the interdigitation of side chains between adjacent filaments and results in looser fibril packing.[45,46] The altered fibril packing and newly formed salt bridges leave unpaired charges on the surface of αS fibrils. In addition, ANS fluorescence (Figure 1G, H) suggests that the E46K mutation increases the solvent exposure of hydrophobic sites in the fibrils. These changes in fibril surface properties suggest the hypothesis that the E46K mutation alters how αS fibrils interact with and recruit αS monomers.

The hypothesis that E46K affects αS monomer-fibril interactions is consistent with the observation that E46K fibrils exhibit greater capacity to seed and cross-seed the formation of nascent aggregates compared to wt.[45,49] In addition, in the context of self-association by domain-swapping, strengthening intramolecular contacts, as in the case of "closed" monomers stabilized by E46K, can also strengthen intermolecular contacts between E46K monomers, thus promoting self-association. However, several questions remain open. For example, how does E46K remodel the network of residues involved in αS monomer-fibril recognition? To what extent do the remodeled monomer-fibril interactions perturb the open *vs* closed equilibrium of αS monomers? Does the E46K mutation also affect early αS self-association that occurs prior to fibril formation? To address these questions, we prepared both WT and E46K αS in their monomeric and fibrillar forms and used NMR to map at atomic resolution the intra- and inter-molecular interactions controlling αS self-association.

Our results reveal that the E46K mutation accelerates αS aggregation by enhancing both primary nucleation αS and late-stage self-association monomer-fibril interactions. The latter enables the mutated fibrils to act as effective allosteric effectors that drive the closed-to-open transition of αS monomers, offsetting the open-to-closed shift observed for E46K αS monomers in the absence of fibrils. The resulting model reconciles the open-to-closed αS monomer shift caused by E46K (Figures 1C and S1) with the amplified propensity for aggregation observed for this mutant (Figure 1D−F). In addition, the proposed model highlights the importance of evaluating the effect of familial mutations not only on the limiting states of the aggregation cascades (*i.e.*, monomers and fibrils), but also on the intermediate species (*e.g.*, early oligomers and monomer-fibril complexes), providing a new perspective on the mechanism of action for a representative hereditary PD- and LBD-related mutation.

RESULTS AND DISCUSSION

The E46K Mutation Promotes Early αS Monomer-Monomer Interactions and Remodels Monomer−Fibril Recognition

The effect of the E46K mutation on early self-association and on monomer-fibril interactions was probed through inter-

https://doi.org/10.1021/jacsau.3c00655
JACS Au 2023, 3, 3485−3493

molecular PREs (Figure 2A, B) and changes in ^{15}N transverse relaxation rates (^{15}N-R_2) upon the addition of preformed fibrils

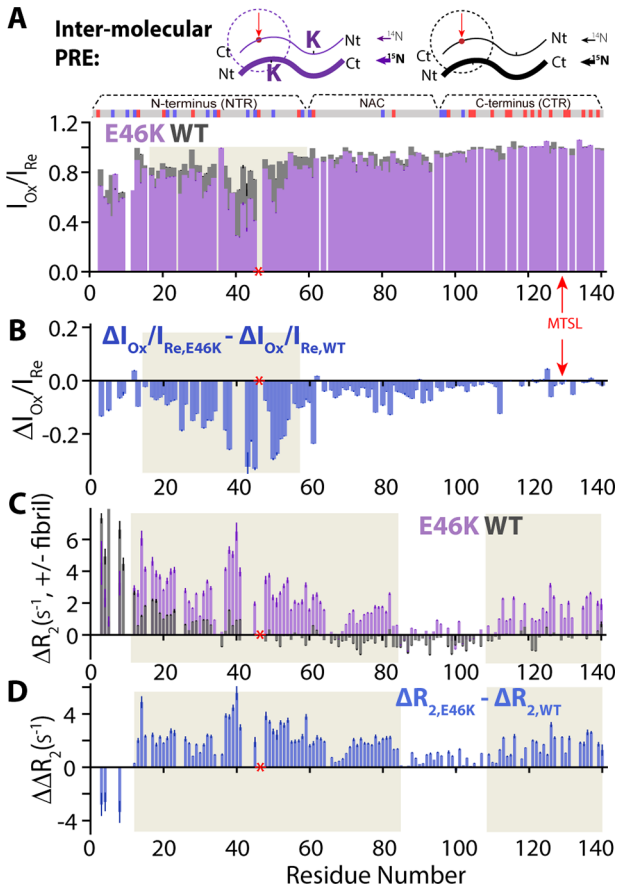

Figure 2. Effect of E46K on transient αS monomer−monomer and monomer-fibril interactions. (A) NMR intermolecular PRE quantified through intensity ratios of oxidized and reduced intensities for 300 μM spin-labeled ^{14}N-labeled αS monomers mixed with 300 μM nonspin-labeled ^{15}N-labeled αS monomers. Black: wt αS; Purple: E46K αS. The site where the MTSL is located is labeled with a red arrow, and the site of the mutation is labeled as a red star. (B) Difference between the PRE ratios of E46K and wt αS in panel A. (C) Differences between the residue-specific ^{15}N-R_2 of 250 μM αS in the presence and absence of 3-fold molar-excess of αS fibrils. Black: wt αS monomers and wt fibrils; Purple: E46K αS monomers and E46K fibrils. (D) Difference between the ΔR_2 profiles in C of E46K and wt. The charge of each amino acid along the sequence is listed on the top with a red (blue, gray) bar representing a negative (positive, neutral) charge. Light gray regions highlight E46K *vs* wt differences.

(Figure 2C, D), respectively. The PRE is a sensitive approach to probing long-range contacts with a paramagnetic spin-label. We attached the spin label to position 129 through a thiol linkage. When this unpaired electron is in close spatial proximity to another atom, the relaxation rate of that atom will be significantly enhanced, and the signal for that atom will be reduced in the NMR spectrum in a manner that is dependent on the proximity of that atom to that spin label. The intermolecular PREs were measured between spin-labeled ^{14}N-αS (which is not detectable by ^{1}H,^{15}N HSQC) and nonspin-labeled ^{15}N-αS (which is detectable by ^{1}H,^{15}N HSQC). The wt αS monomers recognize other wt αS monomers primarily through interactions of the CTR of one chain, where the PRE spin-label is located, with the NTR of another chain, especially residues 40−50 (Figure 2A), consistent with previous intermolecular PRE data obtained with spin-labels at different positions.[14] E46K amplifies these CTR/NTR intermolecular interactions (Figure 2A, B), pointing to enhanced head-to-tail electrostatic attraction arising from the +2 charge increase in the NTR. To evaluate if the E46K charge also affects monomer-fibril interactions, we measured the change in ^{15}N-R_2 rates of wt (E46K) αS upon the addition of wt (E46K) αS preformed fibrils (Figures 2C, S1, and S3). The enhancement in ^{15}N-R_2 rates upon fibril addition indicates a locally increased tumbling time of αS monomers when bound to the fibrils.

While wt αS monomers bind wt αS fibrils primarily through their N-terminus (Figure 2C), as previously reported,[25,26] the E46K mutation markedly remodels this interaction pattern. Notably, the interactions of E46K fibrils with the extreme N-terminus of E46K monomers are significantly attenuated (residues ∼1 to 10 in Figure 2C, D). This loss is compensated by a dramatic enhancement of interactions at several other regions of E46K αS monomers, including the NTR and CTR and, to some extent, also the NAC (gray regions; Figure 2C, D). Similar to the early αS self-association, this pattern is consistent with the E46K mutation enhancing electrostatic intermolecular interactions. The positive charge introduced by the E46K mutation in the αS monomers favors interactions with the negatively charged CTR of the fibrils. In addition, the positive charges introduced by the E46K mutations in the αS fibrils favor interactions with the CTR of the αS monomers. The enhanced electrostatic monomer-fibril interactions also promote fibril engagement of the monomer NAC region in E46K (Figure 2C, D). This is in stark contrast with wt αS for which monomer residues interacting with fibrils are confined to the NTR (Figure 2C) even at fibril saturation conditions (Figure 2C).[25] This observation indicates that the enhanced involvement of the monomer's NAC and CTR regions in fibril bindings (Figure 2C) is an inherent property of the E46K αS independent of the fraction of monomer bound to fibrils. Hence, the extensive monomer-fibril contacts observed for E46K αS may drive a pronounced closed-to-open shift in E46K monomers, which makes them more accessible to fibrils. To test this hypothesis, we evaluated the effect of adding preformed fibrils on the conformation of both wt and E46K αS monomers, as probed through intramolecular PREs (Figure 3).

The E46K Mutation Amplifies the Ability of αS Fibrils to Allosterically Drive the Closed-to-Open Transition of αS Monomers, Exposing Their Aggregation-Prone NAC Region

Wt αS fibrils preferentially interact with open *vs* closed αS monomer conformations, thus allosterically increasing the solvent exposure of the monomers' NAC region, which becomes available for self-association. These results for wt αS are in agreement with previous PRE data obtained using a spin-label in the NAC region.[25] Addition of E46K fibrils markedly amplifies this allosteric effect, as shown by the significantly larger fibril-induced change in PRE effects observed for the NAC region of E46K compared to the WT (Figure 3A−F). Interestingly, such amplification occurs in the NTR and NAC regions (Figure 3E), which are critical for mutated monomers to recognize mutated fibrils (Figure 2D). Furthermore, exposure of the N-terminal and NAC region has also been shown to promote aggregation.[50] The enhanced

https://doi.org/10.1021/jacsau.3c00655
JACS Au 2023, 3, 3485−3493

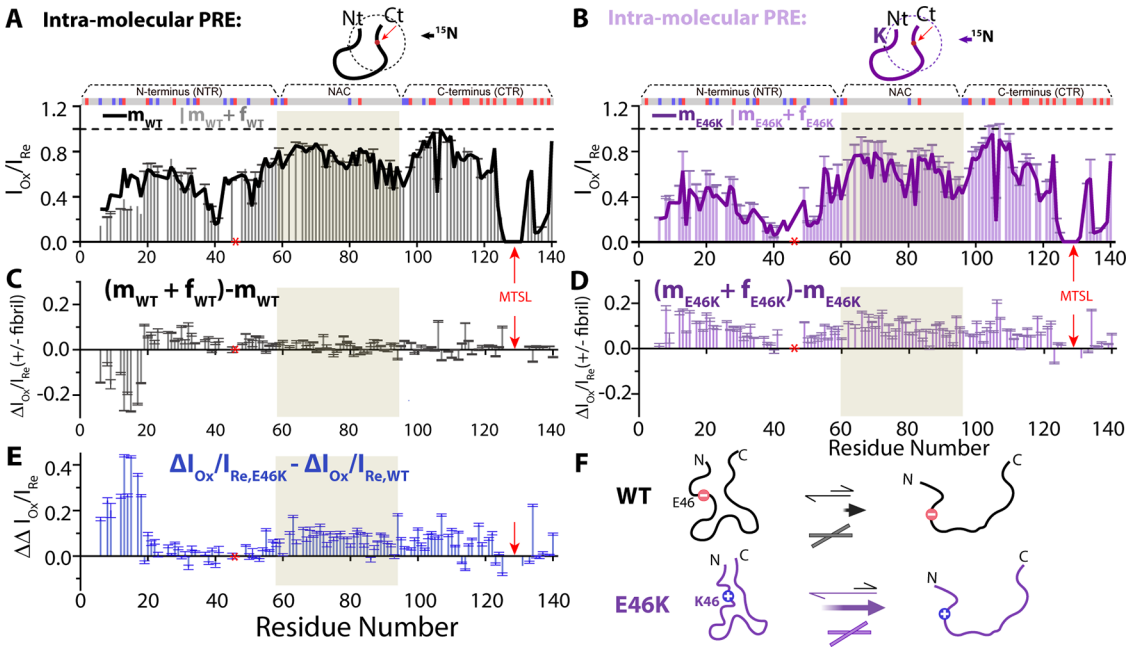

Figure 3. E46K mutation amplifies the closed-to-open shift induced by αS fibril in αS monomers. (A) Intramolecular PREs as quantified by the ratios of oxidized and reduced intensities for 120 μM spin-labeled ^{15}N wt αS monomer in the absence and presence of 3-fold excess unlabeled wt αS fibrils without spin-label. (B) As A but for αS E46K. (C) Difference between the PRE profiles in A. (D) As C but for E46K. (E) Difference between the PRE differentials in C and D. The light gray background region highlights PRE changes occurring in the NAC region. (F) Scheme illustrating fibril-induced closed-to-open monomer shifts.

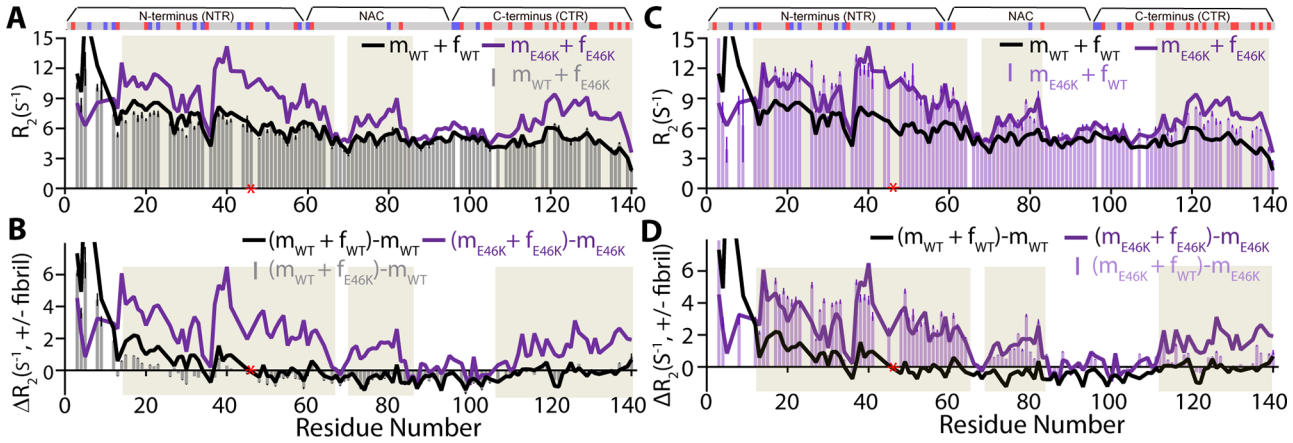

Figure 4. Transient αS monomer-fibril heterointeractions. (A) Residue-specific ^{15}N-R_2 relaxation rates of 250 μM wt αS monomers in the presence of 3-fold excess E46K αS fibrils. ^{15}N-R_2 data from homomixtures is included for the convenience of comparison. (B) As A after subtracting monomer rates. (C, D) As panels A and B, but swapping wt and E46K, *i.e.*, E46K monomer in the presence of 3-fold excess wt αS fibrils. Light gray background highlights key differences between line and bar plots in parts (C) and (D).

E46K monomer opening induced by the mutated fibrils is quite remarkable because the E46K monomers are more compact than the wt monomers in the absence of fibrils (Figures 1C, S1, and 3A, B). Overall, these observations suggest that the enhanced monomer-fibril interactions in E46K αS at least partially offset the mutation-induced strengthening of intramolecular NTR/CTR interactions typical of closed αS conformers (Figure 3F). They also highlight the critical role of the monomer-fibril complex in evaluating the effect of PD-related mutations. To dissect the relative contributions of E46K mutations in αS monomers *vs* fibrils, we extended the ^{15}N relaxation experiments of Figure 2C, D to heteromixtures of wt monomers and mutant fibrils and *vice versa* (Figure 4).

Furthermore, E46K is a heterozygous αS mutation, and its effect on PD is amplified by wt αS.[35,49,51]

The E46K Monomer Mutation Alone Is Necessary and Sufficient to Drive Fibril Interactions with the Monomer NTR and NAC Regions, While Fibril Interactions with the Monomer CTR Region Require the E46K Mutation to be Present in Both the Monomer and Fibrils

The ^{15}N-R_2 values for wt monomers in the presence of E46K fibrils (Figure 4A, B, gray bars) are markedly reduced compared to those measured for E46K monomers in the presence of E46K fibrils (Figure 4A, purple line) and resemble quite closely those observed for wt monomers in the presence of wt fibrils (Figure 4A, black line). This observation indicates that the monomer E46K mutation is necessary to enhance the

https://doi.org/10.1021/jacsau.3c00655
JACS Au 2023, 3, 3485−3493

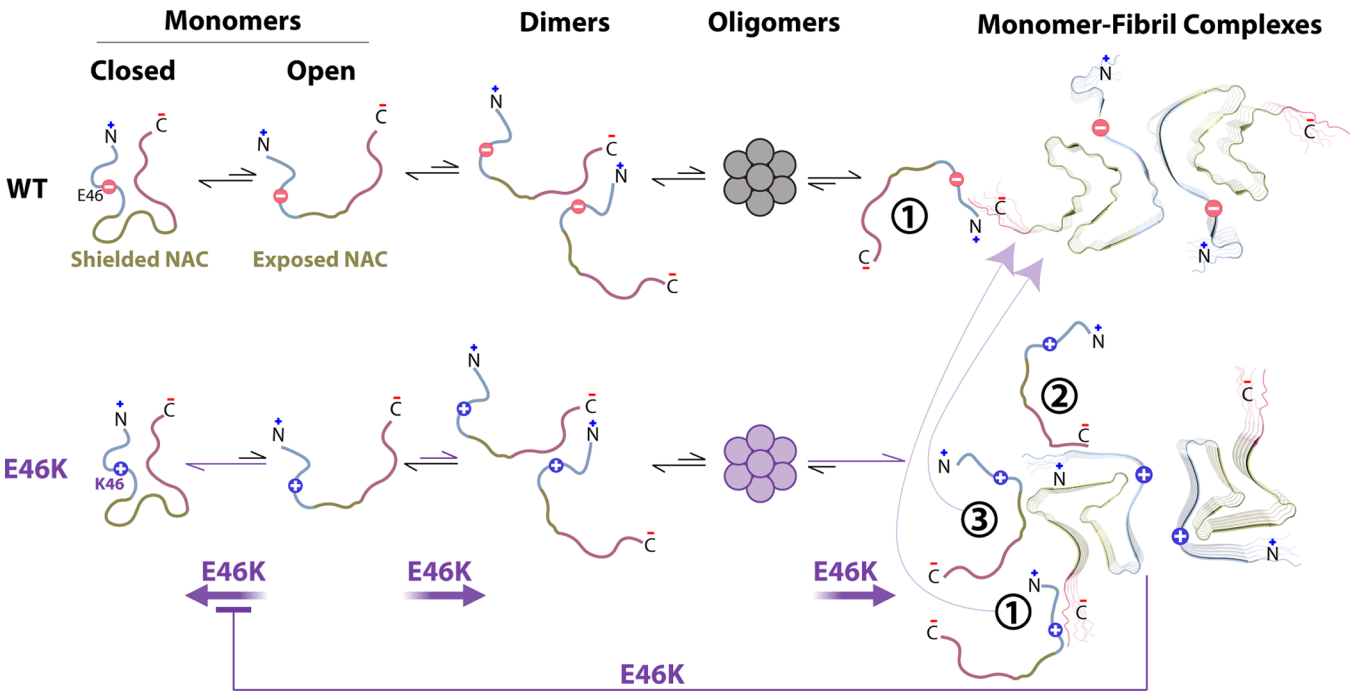

Figure 5. Proposed multipronged mechanism of action for the early onset PD mutation E46K. Key self-association equilibria and interactions perturbed by E46K are illustrated for both wt and E46K αS. The mutation acts at multiple levels (purple arrows and lines) and results in new types of monomer-fibril recognition modes denoted as 1−3 and involving monomers' NTR, CTR and NAC regions, respectively. Modes 1 and 3 apply to both wt and mutant fibrils, as indicated by the curved arrows. The wt mechanism agrees with previous findings.[16,25] Fibril structures are adapted from PDB structures 6CU7 and 6UFR for WT and E46K fibrils,[36,44] respectively. N- and C- termini are depicted as disordered lines.

monomer-fibril interactions. On the contrary, the ^{15}N-R_2 values for E46K monomers in the presence of wt fibrils (Figure 4C, D, purple bars) remain quite similar to those measured for E46K monomers in the presence of E46K fibrils, with the exception of select C-terminal residues.

While the transient monomer-fibril interactions probed through NMR relaxation changes are often insufficient to report on the full complexity of seeding experiments, the comparison of results from the homo- *vs* hetero- monomer-fibril mixtures (Figures 2C, D and 4) help dissect the relative contributions of monomer *vs* fibril mutations to monomer-fibril recognition and lead to two major implications. First, the monomer E46K mutation is not only necessary but also sufficient alone to enhance monomer NTR and NAC region-fibril interactions, irrespective of whether the fibrils are wt or E46K. Second, the monomer CTR engages in fibril interactions only when the E46K mutation occurs in both monomer and fibrils, in stark contrast with the NTR and NAC regions. A possible explanation is that the negatively charged CTR of αS monomers is recruited by positive charges in the mutated fibrils exposed through the salt-bridge rewiring triggered by the E46K mutation (Figure S4).[36,44] Overall, the E46K mutations in both αS monomers and fibrils cause a drastic remodeling of monomer-fibril interactions, which play a central role in the mechanism of action for this PD-related αS mutant.

CONCLUSIONS

In summary, based on our results, we propose a multipronged mechanism of action for the E46K early-onset PD-related mutation. Our comparative E46K *vs* wt analyses (Figures 1−4) reveal that the E46K mutation amplifies αS aggregation by affecting the αS self-association cascade at multiple levels (Figure 5). The E46K mutation perturbs not only the monomer and fibril end points (Figures 1C−H and S2),[8,11−13,36−41,50,52,53] but also several intermediate equilibria (Figure 5). Besides causing a shift of αS to aggregation-averse closed conformers and a major rewiring of salt-bridges in αS fibrils,[36,44−46] E46K perturbs both early- and late- stage self-association interactions. It enhances primary-nucleation of αS monomers through head-to-tail NTR-CTR intermolecular interactions (Figures 2A,B and 5) as well as late-stage self-association through αS monomer-fibril binding (Figures 2C,D and 5). The enhancement of monomer-fibril interactions involves not only the potentiation of select contacts already observed for wt αS (recognition mode one, Figure 5), but also introduces two new monomer-fibril recognition modes not observed for wt αS (Figure 2C,D; recognition modes two and three, Figure 5). In recognition mode one, fibrils target primarily the NTR of E46K αS monomers, albeit weaken the engagement of the first ten residues observed for wt αS monomers (Figure 2C,D). In modes two and three fibrils contact E46K αS monomers mainly through the CTR and NAC regions (Figures 2C,D and5) that are fully disengaged in wt αS monomers (Figures 2C,D and 5). Interestingly, recognition modes one and three are largely preserved when E46K monomers bind to wt fibrils (Figures 4C, D and 5). However, mode two requires both the monomer and fibrils to be mutated. Recognition modes one and two are also supported by previous MD simulations showing that the E46K mutation makes the N- and C-termini more reactive toward fibrillization.[37] In addition, other molecular modeling studies[54] reported that E46K makes NAC residues 68−78 more aggregation prone, consistent with recognition mode three (Figure 5).

https://doi.org/10.1021/jacsau.3c00655
JACS Au 2023, 3, 3485−3493

Collectively, monomer-fibril binding interactions are relevant not only for αS fibril elongation and secondary nucleation,[24−26,55] but also for the αS fibrils to function as allosteric effectors that drive close-to-open αS monomer transitions (Figures 3 and 5). These fibril-induced transitions counter the stabilization of closed conformers elicited by the mutation in the absence of fibrils (Figure 1C), and together with the enhanced monomer−monomer and monomer-fibril interactions (Figure 5), explain how the E46K mutation accelerates the kinetics of αS aggregation (Figure 1D), in line with the known clinical phenotype of early onset PD and LBDs. However, it will be important to complement our experimental results by expanding the previous modeling work on E46K[37,54,56] to include simulations of how αS fibrils induce closed-to-open shifts in wt and E46K monomers.

EXPERIMENTAL PROCEDURES

Alpha Synuclein Site-Directed Mutagenesis

The plasmid for E46K mutation was purchased from Addgene (#105728), while the S129C and S129C/E46K plasmids were generated through site-directed mutagenesis. All constructs were verified by DNA sequencing.

Alpha Synuclein Expression and Purification

The αS WT and mutants were expressed in *E. coli* BL21(DE3) cells, as described before[57−59] Further details can be found in the Supporting Information under experimental procedures.

Size Exclusion Chromatograph and Multi-angle Light Scattering (SEC-MALS)

SEC-MALS experiments were acquired as previously reported, using a Superdex 200 increase 10/300 analytical gel filtration column and a Wyatt miniDAWN MALS detector in 50 mM HEPES pH 7.4 in the 4 °C fridge.[59]

Fibril Preparation

For the preparation of mature fibrils, fresh unlabeled WT and E46K αS monomer samples were equilibrated into 1 × PBS (137 mM NaCl, 2.7 mM KCl, 8 mM Na_2HPO_4, and 2 mM KH_2PO_4, dilute from 10× Phosphate Buffered Saline from BioShop Lot No.:9F61076) pH 7.4 buffer containing 0.05% NaN_3 after the anion exchange filtration with SEC column (HiLoad 16/60 Superdex 200 gel filtration column, GE healthcare). αS monomers were concentrated to 500 μM, aliquoted into 0.5 mL volumes per Eppendorf tube, and incubated in a 37 °C shaker for 4 weeks at 200 rpm. To remove the salts, fibrils were pelleted by ultracentrifuge at 121,968 *g* and washed with NMR buffer three times. The fibril concentration was determined by using absorbance at 280 nm in the presence of 8 M urea.

Thioflavin T (ThT) Fluorescence Measurements

To measure the aggregation kinetic of αS variants, fresh unlabeled monomer samples were prepared and equilibrated into 20 mM K_2HPO_4, 5 mM KH_2PO_4, 100 mM KCl, and 0.05% NaN_3. 300 μM unlabeled αS variants were incubated with 10 μM ThT at 37 °C, shaking at 400 rpm for 30 s before each measurement. Fluorescence measurements were acquired in triplicated wells using a Biotek Cytation 5 plate-reader with excitation and emission wavelengths of 450 and 485 nm, respectively.

Spin Labeling of Alpha Synuclein

The reaction of αS cysteine mutants with the nitroxide spin-label MTSL (1-oxyl-2,2,5,5-tetramethyl−3-pyrroline-3-methylmethanethiosulfonate; Toronto Research Chemicals Inc.) was performed as described previously.[16] Briefly, the lyophilized αS was dissolved into 50 mM HEPES pH 7.4 buffer and incubated with six−fold molar excess DTT for 30 min at room temperature. The excess DTT was subsequently removed using a series of 5 mL (×3) HiTrap desalting columns (Sigma-Aldrich GE17-1408-01). 10-fold molar excess of MTSL was immediately added to the protein solution and incubated for 4 h at room temperature in the dark. To remove high-molecular-weight αS and excess MTSL, the reacted sample was loaded onto a SEC column (HiLoad 16/60 Superdex 200 gel filtration column, GE Healthcare) equilibrated with 0.02% NaN_3 dd H_2O. The efficiency of the MTSL attachment was determined by evaluating the free thiol concentration through the DTNB assay before and after the MTSL reaction.[60] The monomeric αS-MTSL conjugate was aliquoted, lyophilized into powder, and stored at −20 °C. The spin-label positions in this study were chosen considering that the same or similar spin-label positions were previously shown to be minimally invasive and suitable to investigate inter- and intra-molecular interactions.[14,60−62]

Dynamic Light Scattering (DLS)

After ultracentrifugation, wt and E46K fibril pellets were resuspend into a 50 mM HEPES, pH 7.4, buffer to a final concentration of 300 μM. The samples were loaded into 40 μL (ZEN0040) plastic cuvettes. DLS measurements were performed at 10 °C by using a Zetasizer Nano ZS Instrument (Malvern Instruments, Malvern UK). The viscosity value for water was used in the analysis of all measurements. Error bars are based on the standard deviation of five replicates.

Negative Stain Electron Microscopy (EM)

Wt and E46K fibril pellets were resuspended into dd H_2O to a final concentration of 10 μM. Copper EM grids (400-mesh) coated with a continuous layer of amorphous carbon were glow discharged with a 5-mA current for 15 s. Three μL of fibrils was added on the grid. After 1 min, the excess of sample was blotted, and the grids were stained with 1% uranyl acetate for 30 s. EM images were acquired with a JEOL 1200-EX electron microscope operated at 80 kV as in previous studies.[57]

NMR Spectroscopy

All NMR samples were prepared by dissolving the αS lyophilized powder in 50 mM HEPES buffer at pH 7.4 with 5% D_2O on ice and transferred into 3 mm NMR tubes. All spectra were analyzed with TopSpin 4.1.4 and NMRFAM Sparky. The sample concentrations were 250 μM for monomers and 750 μM for fibrils. $^1H-^{15}N$ HSQC spectra were recorded with eight scans, 2K (t_2) and 180 (t_1) complex points for spectral widths of 16.23 (^1H) and 35.00 ppm (^{15}N), respectively. ^{15}N-Transverse relaxation data were acquired with a Bruker NEO 700 spectrometer equipped with a TCI cryo-probe at 283 K, using a pseudo-3D pulse sequence as described previously and CPMG durations of 31.36, 62.72, 94.08, 125.44, and 156.80, 188.16 ms.[59] The ^{15}N-transverese relaxation spectra were recorded with 16 scans, 2K (t_2) and 300 (t_1) complex points for spectral widths of 13.73 ppm (^1H) and 38.00 ppm (^{15}N), respectively. Unresolved peaks were excluded from further analyses. $^1H-^{15}N$ HSQC spectra for paramagnetic relaxation enhancement (PRE) experiments were acquired with a Bruker 850 HD spectrometer equipped with a TCI cryo-probe at 283 K. The sample concentrations were 120 μM for monomers and 360 μM for fibrils. The oxidized and reduced state spectra for αS-MTSL samples were acquired with 12 scans and 2K (t2) and 256 (t1) complex points for spectral widths of 15.98 ppm (^1H) and 35.00 ppm (^{15}N), respectively. To reduce the spin label, ascorbic acid was added to the oxidized NMR sample at a final concentration of 2 mM, without significantly changing the volume or pH, and incubated for 1 h at room temperature. Aggregation during PRE experiments was ruled out by running controls without MTSL αS in the presence of fibrils.

1-Anilino-8-napthalenesulfonate (ANS) Fluorescence

The αS fibril stocks were prepared as for NMR experiments by resuspension into 50 mM HEPES buffer at pH 7.4. The final concentration for fluorescence was 250 μM. ANS was diluted from a DMSO stock into 50 mM HEPES buffer at pH 7.4 with αS fibrils to a final concentration of 50 μM. The final concentration of DMSO in the sample was 0.025% and had no significant effect on the measurements. The control was a solution with ANS to rule out background fluorescence. The data were acquired using a Biotek Cytation 5 plate reader with an excitation wavelength of 350 nm and

https://doi.org/10.1021/jacsau.3c00655
JACS Au 2023, 3, 3485−3493

emission wavelength from 400 to 600 nm (465 and 485 nm as maximum emission fluorescence were also separately acquired). Triplicate wells were used for each sample, and duplicate acquisitions were conducted for each well, with a total of six data points. The scanned fluorescence data were normalized to the maximum fluorescence, and the control was subtracted for each wavelength. The end point fluorescence data were normalized to the maximum fluorescence among both emission wavelengths.

■ ASSOCIATED CONTENT

Supporting Information

The Supporting Information is available free of charge at https://pubs.acs.org/doi/10.1021/jacsau.3c00655.

Experimental details of sample preparation and fibril surface analyses as well as four figures; additional NMR relaxation data in the absence and presence of fibrils; and further DLS and fibril surface characterizations (PDF)

■ AUTHOR INFORMATION

Corresponding Author

Giuseppe Melacini − *Department of Chemistry and Chemical Biology, McMaster University, Hamilton, ON L8S 4M1, Canada;* orcid.org/0000-0003-1164-2853; Email: melacin@mcmaster.ca

Authors

Jinfeng Huang − *Department of Chemistry and Chemical Biology, McMaster University, Hamilton, ON L8S 4M1, Canada;* orcid.org/0000-0002-6342-8536

Rashik Ahmed − *Department of Chemistry and Chemical Biology, McMaster University, Hamilton, ON L8S 4M1, Canada*

Madoka Akimoto − *Department of Chemistry and Chemical Biology, McMaster University, Hamilton, ON L8S 4M1, Canada*

Karla Martinez Pomier − *Department of Chemistry and Chemical Biology, McMaster University, Hamilton, ON L8S 4M1, Canada*

Complete contact information is available at: https://pubs.acs.org/10.1021/jacsau.3c00655

Author Contributions

J.H. designed, executed the experiments, analyzed all the data, and wrote the manuscript, R.A. designed the experiments and discussed the results; M.A. helped conduct the SEC-MALS experiment and discuss the conclusions; K.M.P. contributed to the discussion of the results, G.M. contributed to the design of the experiments, the analysis of the data and the writing of the manuscript. All authors have edited and given approval to the final version of the manuscript.

Funding

This work was supported by the Natural Sciences and Engineering Research Council of Canada Grant RGPIN-2019-05990 (to G. M.).

Notes

The authors declare no competing financial interest.

■ ACKNOWLEDGMENTS

We thank Qiulin Ma, Leonardo Della Libera, Mariia Khamina, and Evelyn Kamski-Hennekam for helpful discussions.

■ ABBREVIATIONS

αS, alpha synuclein; WT, wildtype; NMR, nuclear magnetic resonance; NTR, N- termini; CTR, C-termini; NAC, non-amyloid β component; PREs, aramagnetic relaxation enhancements

■ REFERENCES

(1) Spillantini, M. G.; Schmidt, M. L.; Lee, V. M.-Y.; Trojanowski, J. Q.; Jakes, R.; Goedert, M. α-Synuclein in Lewy bodies. *Nature* **1997**, *388* (6645), 839−840.

(2) Cohen, A. S.; Calkins, E. Electron microscopic observations on a fibrous component in amyloid of diverse origins. *Nature* **1959**, *183* (4669), 1202−1203.

(3) Singleton, A. B.; Farrer, M.; Johnson, J.; Singleton, A.; Hague, S.; Kachergus, J.; Hulihan, M.; Peuralinna, T.; Dutra, A.; Nussbaum, R.; et al. α-Synuclein Locus Triplication Causes Parkinson's Disease. *Science* **2003**, *302* (5646), 841−841.

(4) Chiti, F.; Dobson, C. M. Protein Misfolding, Amyloid Formation, and Human Disease: A Summary of Progress Over the Last Decade. *Annu. Rev. Biochem.* **2017**, *86* (1), 27−68.

(5) Baba, M.; Nakajo, S.; Tu, P. H.; Tomita, T.; Nakaya, K.; Lee, V. M.; Trojanowski, J. Q.; Iwatsubo, T. Aggregation of alpha-synuclein in Lewy bodies of sporadic Parkinson's disease and dementia with Lewy bodies. *Am. J. Pathol.* **1998**, *152* (4), 879−884.

(6) Lee, H.-J.; Bae, E.-J.; Lee, S.-J. Extracellular α-synuclein—a novel and crucial factor in Lewy body diseases. *Nat. Rev. Neurol.* **2014**, *10* (2), 92−98.

(7) Fusco, G.; Chen, S. W.; Williamson, P. T. F.; Cascella, R.; Perni, M.; Jarvis, J. A.; Cecchi, C.; Vendruscolo, M.; Chiti, F.; Cremades, N.; et al. Structural basis of membrane disruption and cellular toxicity by alpha-synuclein oligomers. *Science* **2017**, *358* (6369), 1440−1443.

(8) Choi, W.; Zibaee, S.; Jakes, R.; Serpell, L. C.; Davletov, B.; Crowther, R. A.; Goedert, M. Mutation E46K increases phospholipid binding and assembly into filaments of human alpha-synuclein. *FEBS Lett.* **2004**, *576* (3), 363−368.

(9) Pandey, N.; Schmidt, R. E.; Galvin, J. E. The alpha-synuclein mutation E46K promotes aggregation in cultured cells. *Exp. Neurol.* **2006**, *197* (2), 515−520.

(10) Lazaro, D. F.; Rodrigues, E. F.; Langohr, R.; Shahpasandzadeh, H.; Ribeiro, T.; Guerreiro, P.; Gerhardt, E.; Krohnert, K.; Klucken, J.; Pereira, M. D.; et al. Systematic Comparison of the Effects of Alpha-synuclein Mutations on Its Oligomerization and Aggregation. *PLoS Genet.* **2014**, *10* (11), No. 1004741.

(11) Greenbaum, E. A.; Graves, C. L.; Mishizen-Eberz, A. J.; Lupoli, M. A.; Lynch, D. R.; Englander, S. W.; Axelsen, P. H.; Giasson, B. I. The E46K mutation in alpha-synuclein increases amyloid fibril formation. *J. Biol. Chem.* **2005**, *280* (9), 7800−7807.

(12) Bhattacharyya, D.; Kumar, R.; Mehra, S.; Ghosh, A.; Maji, S. K.; Bhunia, A. Multitude NMR studies of alpha-synuclein familial mutants: probing their differential aggregation propensities. *Chem. Commun.* **2018**, *54* (29), 3605−3608.

(13) Meena, V. K.; Kumar, V.; Karalia, S. Garima; Sundd, M. Ellagic Acid Modulates Uninduced as well as Mutation and Metal-Induced Aggregation of α-Synuclein: Implications for Parkinson's Disease. *ACS Chem. Neurosci.* **2021**, *12* (19), 3598−3614.

(14) Wu, K.-P.; Baum, J. Detection of Transient Interchain Interactions in the Intrinsically Disordered Protein alpha-Synuclein by NMR Paramagnetic Relaxation Enhancement. *J. Am. Chem. Soc.* **2010**, *132* (16), 5546−5547.

(15) Bertoncini, C. W.; Jung, Y. S.; Fernandez, C. O.; Hoyer, W.; Griesinger, C.; Jovin, T. M.; Zweckstetter, M. Release of long-range tertiary interactions potentiates aggregation of natively unstructured alpha-synuclein. *Proc. Natl. Acad. Sci. U.S.A.* **2005**, *102* (5), 1430−1435.

(16) Dedmon, M. M.; Lindorff-Larsen, K.; Christodoulou, J.; Vendruscolo, M.; Dobson, C. M. Mapping long-range interactions in alpha-synuclein using spin-label NMR and ensemble molecular dynamics simulations. *J. Am. Chem. Soc.* **2005**, *127* (2), 476−477.

(17) Allison, J. R.; Varnai, P.; Dobson, C. M.; Vendruscolo, M. Determination of the Free Energy Landscape of alpha-Synuclein Using Spin Label Nuclear Magnetic Resonance Measurements. *J. Am. Chem. Soc.* **2009**, *131* (51), 18314−18326.
(18) Porcelli, F.; Buck-Koehntop, B. A.; Thennarasu, S.; Ramamoorthy, A.; Veglia, G. Structures of the Dimeric and Monomeric Variants of Magainin Antimicrobial Peptides (MSI-78 and MSI-594) in Micelles and Bilayers Determined by NMR Spectroscopy. *Biochemistry* **2006**, *45* (18), 5793−5799.
(19) Tavassoly, O.; Nokhrin, S.; Dmitriev, O. Y.; Lee, J. S. Cu(II) and dopamine bind to α-synuclein and cause large conformational changes. *FEBS J.* **2014**, *281* (12), 2738−2753.
(20) Bickers, S. C.; Sayewich, J. S.; Kanelis, V. Intrinsically disordered regions regulate the activities of ATP binding cassette transporters. *Biochim. Biophys. Acta - Biomembr.* **2020**, *1862* (6), No. 183202.
(21) Ahmed, R.; Melacini, G. A solution NMR toolset to probe the molecular mechanisms of amyloid inhibitors. *Chem. Commun.* **2018**, *54* (37), 4644−4652.
(22) Martinez Pomier, K.; Ahmed, R.; Melacini, G. Catechins as Tools to Understand the Molecular Basis of Neurodegeneration. *Molecules* **2020**, *25* (16), 3571.
(23) Huang, H.; Milojevic, J.; Melacini, G. Analysis and Optimization of Saturation Transfer Difference NMR Experiments Designed to Map Early Self-Association Events in Amyloidogenic Peptides. *J. Phys. Chem. B* **2008**, *112* (18), 5795−5802.
(24) Gaspar, R.; Meisl, G.; Buell, A. K.; Young, L.; Kaminski, C. F.; Knowles, T. P. J.; Sparr, E.; Linse, S. Secondary nucleation of monomers on fibril surface dominates α-synuclein aggregation and provides autocatalytic amyloid amplification. *Q. Rev. Biophys.* **2017**, *50*, No. e6.
(25) Kumari, P.; Ghosh, D.; Vanas, A.; Fleischmann, Y.; Wiegand, T.; Jeschke, G.; Riek, R.; Eichmann, C. Structural insights into alpha-synuclein monomer-fibril interactions. *Proc. Natl. Acad. Sci. U.S.A.* **2021**, *118* (10), No. e2012171118.
(26) Yang, X.; Wang, B.; Hoop, C. L.; Williams, J. K.; Baum, J. NMR unveils an N-terminal interaction interface on acetylated-alpha-synuclein monomers for recruitment to fibrils. *Proc. Natl. Acad. Sci. U.S.A.* **2021**, *118* (18), No. e2017452118.
(27) Suzuki, Y.; Brender, J. R.; Hartman, K.; Ramamoorthy, A.; Marsh, E. N. G. Alternative Pathways of Human Islet Amyloid Polypeptide Aggregation Distinguished by 19F Nuclear Magnetic Resonance-Detected Kinetics of Monomer Consumption. *Biochemistry* **2012**, *51* (41), 8154−8162.
(28) Krishnamoorthy, J.; Brender, J. R.; Vivekanandan, S.; Jahr, N.; Ramamoorthy, A. Side-Chain Dynamics Reveals Transient Association of Aβ1−40 Monomers with Amyloid Fibers. *J. Phys. Chem. B* **2012**, *116* (46), 13618−13623.
(29) Brender, J. R.; Ghosh, A.; Kotler, S. A.; Krishnamoorthy, J.; Bera, S.; Morris, V.; Sil, T. B.; Garai, K.; Reif, B.; Bhunia, A.; Ramamoorthy, A. Probing transient non-native states in amyloid beta fiber elongation by NMR. *Chem. Commun.* **2019**, *55* (31), 4483−4486.
(30) Wang, C. Solution NMR Studies of Aβ Monomers and Oligomers. In *Protein and Peptide Folding, Misfolding, and Non-Folding*; Wiley, 2012; pp. 389−411.
(31) Pham, N. T. H.; Létourneau, M.; Fortier, M.; Bégin, G.; Al-Abdul-Wahid, M. S.; Pucci, F.; Folch, B.; Rooman, M.; Chatenet, D.; St-Pierre, Y.; et al. Perturbing dimer interactions and allosteric communication modulates the immunosuppressive activity of human galectin-7. *J. Biol. Chem.* **2021**, *297* (5), No. 101308.
(32) Xu, L.; Ma, B.; Nussinov, R.; Thompson, D. Familial Mutations May Switch Conformational Preferences in α-Synuclein Fibrils. *ACS Chem. Neurosci.* **2017**, *8* (4), 837−849.
(33) Buratti, F. A.; Boeffinger, N.; Garro, H. A.; Flores, J. S.; Hita, F. J.; Gonçalves, P. D. C.; Copello, F. D. R.; Lizarraga, L.; Rossetti, G.; Carloni, P.; et al. Aromaticity at position 39 in α-synuclein: A modulator of amyloid fibril assembly and membrane-bound conformations. *Protein Sci.* **2022**, *31* (7), No. e4360.
(34) Frieg, B.; Geraets, J. A.; Strohäker, T.; Dienemann, C.; Mavroeidi, P.; Jung, B. C.; Kim, W. S.; Lee, S.-J.; Xilouri, M.; Zweckstetter, M.; Schröder, G. F. Quaternary structure of patient-homogenate amplified α-synuclein fibrils modulates seeding of endogenous α-synuclein. *Commun. Biol.* **2022**, *5* (1), 1040.
(35) Zarranz, J. J.; Alegre, J.; Gómez-Esteban, J. C.; Lezcano, E.; Ros, R.; Ampuero, I.; Vidal, L.; Hoenicka, J.; Rodriguez, O.; Atarés, B. The new mutation, E46K, of α-synuclein causes parkinson and Lewy body dementia. *Ann. Neurol.* **2004**, *55* (2), 164−173.
(36) Boyer, D. R.; Li, B.; Sun, C.; Fan, W.; Zhou, K.; Hughes, M. P.; Sawaya, M. R.; Jiang, L.; Eisenberg, D. S. The alpha-synuclein hereditary mutation E46K unlocks a more stable, pathogenic fibril structure. *Proc. Natl. Acad. Sci. U.S.A.* **2020**, *117* (7), 3592−3602.
(37) Wise-Scira, O.; Dunn, A.; Aloglu, A. K.; Sakallioglu, I. T.; Coskuner, O. Structures of the E46K mutant-type alpha-synuclein protein and impact of E46K mutation on the structures of the wild-type alpha-synuclein protein. *ACS Chem. Neurosci.* **2013**, *4* (3), 498−508.
(38) Rospigliosi, C. C.; McClendon, S.; Schmid, A. W.; Ramlall, T. F.; Barre, P.; Lashuel, H. A.; Eliezer, D. E46K Parkinson's-linked mutation enhances C-terminal-to-N-terminal contacts in alpha-synuclein. *J. Mol. Biol.* **2009**, *388* (5), 1022−1032.
(39) Fongaro, B.; Cappelletto, E.; Sosic, A.; Spolaore, B.; Polverino de Laureto, P. 3,4-Dihydroxyphenylethanol and 3,4-dihydroxyphenyl-acetic acid affect the aggregation process of E46K variant of α-synuclein at different extent: Insights into the interplay between protein dynamics and catechol effect. *Protein Sci.* **2022**, *31* (7), No. e4356.
(40) Ono, K.; Ikeda, T.; Takasaki, J.-i.; Yamada, M. Familial Parkinson disease mutations influence α-synuclein assembly. *Neurobiol. Dis.* **2011**, *43* (3), 715−724.
(41) Sahay, S.; Ghosh, D.; Dwivedi, S.; Anoop, A.; Mohite, G. M.; Kombrabail, M.; Krishnamoorthy, G.; Maji, S. K. Familial Parkinson Disease-associated Mutations Alter the Site-specific Microenvironment and Dynamics of α-Synuclein. *J. Biol. Chem.* **2015**, *290* (12), 7804−7822.
(42) Kamski-Hennekam, E. R.; Huang, J.; Ahmed, R.; Melacini, G. Toward a molecular mechanism for the interaction of ATP with alpha-synuclein. *Chem. Sci.* **2023**, *14* (36), 9933−9942.
(43) Bokor, M.; Házy, E.; Tantos, Á. Wide-Line NMR Melting Diagrams, Their Thermodynamic Interpretation, and Secondary Structure Predictions for A30P and E46K α-Synuclein. *ACS Omega* **2022**, *7* (22), 18323−18330.
(44) Li, B.; Ge, P.; Murray, K. A.; Sheth, P.; Zhang, M.; Nair, G.; Sawaya, M. R.; Shin, W. S.; Boyer, D. R.; Ye, S.; et al. Cryo-EM of full-length α-synuclein reveals fibril polymorphs with a common structural kernel. *Nat. Commun.* **2018**, *9* (1), 3609.
(45) Zhao, K.; Li, Y.; Liu, Z.; Long, H.; Zhao, C.; Luo, F.; Sun, Y.; Tao, Y.; Su, X. D.; Li, D.; et al. Parkinson's disease associated mutation E46K of alpha-synuclein triggers the formation of a distinct fibril structure. *Nat. Commun.* **2020**, *11* (1), 2643.
(46) Guerrero-Ferreira, R.; Taylor, N. M. I.; Mona, D.; Ringler, P.; Lauer, M. E.; Riek, R.; Britschgi, M.; Stahlberg, H. Cryo-EM structure of alpha-synuclein fibrils. *eLife* **2018**, *7*, No. e36402.
(47) Lemkau, L. R.; Comellas, G.; Lee, S. W.; Rikardsen, L. K.; Woods, W. S.; George, J. M.; Rienstra, C. M. Site-specific perturbations of alpha-synuclein fibril structure by the Parkinson's disease associated mutations A53T and E46K. *PLoS One* **2013**, *8* (3), No. e49750.
(48) Harada, R.; Kobayashi, N.; Kim, J.; Nakamura, C.; Han, S. W.; Ikebukuro, K.; Sode, K. The effect of amino acid substitution in the imperfect repeat sequences of alpha-synuclein on fibrillation. *Biochim. Biophys. Acta - Mol. Basis Dis.* **2009**, *1792* (10), 998−1003.
(49) Long, H.; Zheng, W.; Liu, Y.; Sun, Y.; Zhao, K.; Liu, Z.; Xia, W.; Lv, S.; Liu, Z.; Li, D.; et al. Wild-type alpha-synuclein inherits the structure and exacerbated neuropathology of E46K mutant fibril strain by cross-seeding. *Proc. Natl. Acad. Sci. U.S.A.* **2021**, *118* (20), No. e2012435118.

https://doi.org/10.1021/jacsau.3c00655
JACS Au 2023, 3, 3485−3493

(50) Stephens, A. D.; Zacharopoulou, M.; Moons, R.; Fusco, G.; Seetaloo, N.; Chiki, A.; Woodhams, P. J.; Mela, I.; Lashuel, H. A.; Phillips, J. J.; et al. Extent of N-terminus exposure of monomeric alpha-synuclein determines its aggregation propensity. *Nat. Commun.* **2020**, *11* (1), 2820.
(51) Flagmeier, P.; Meisl, G.; Vendruscolo, M.; Knowles, T. P.; Dobson, C. M.; Buell, A. K.; Galvagnion, C. Mutations associated with familial Parkinson's disease alter the initiation and amplification steps of alpha-synuclein aggregation. *Proc. Natl. Acad. Sci. U.S.A.* **2016**, *113* (37), 10328−10333.
(52) Rovere, M.; Powers, A. E.; Jiang, H.; Pitino, J. C.; Fonseca-Ornelas, L.; Patel, D. S.; Achille, A.; Langen, R.; Varkey, J.; Bartels, T. E46K-like alpha-synuclein mutants increase lipid interactions and disrupt membrane selectivity. *J. Biol. Chem.* **2019**, *294* (25), 9799−9812.
(53) Ranjan, P.; Kumar, A. Perturbation in Long-Range Contacts Modulates the Kinetics of Amyloid Formation in α-Synuclein Familial Mutants. *ACS Chem. Neurosci.* **2017**, *8* (10), 2235−2246.
(54) Kumar, S.; Sarkar, A.; Sundar, D. Controlling aggregation propensity in A53T mutant of alpha-synuclein causing Parkinson's disease. *Biochem. Biophys. Res. Commun.* **2009**, *387* (2), 305−309.
(55) Buell, A. K.; Galvagnion, C.; Gaspar, R.; Sparr, E.; Vendruscolo, M.; Knowles, T. P.; Linse, S.; Dobson, C. M. Solution conditions determine the relative importance of nucleation and growth processes in alpha-synuclein aggregation. *Proc. Natl. Acad. Sci. U.S.A.* **2014**, *111* (21), 7671−7676.
(56) Aggarwal, L.; Biswas, P. Hydration Thermodynamics of Familial Parkinson's Disease-Linked Mutants of α-Synuclein. *J. Chem. Inf. Model.* **2021**, *61* (4), 1850−1858.
(57) Hoyer, W.; Antony, T.; Cherny, D.; Heim, G.; Jovin, T. M.; Subramaniam, V. Dependence of α-synuclein aggregate morphology on solution conditions. *J. Mol. Biol.* **2002**, *322* (2), 383−393.
(58) Ahmed, R.; Huang, J.; Weber, D. K.; Gopinath, T.; Veglia, G.; Akimoto, M.; Khondker, A.; Rheinstadter, M. C.; Huynh, V.; Wylie, R. G.; et al. Molecular Mechanism for the Suppression of Alpha Synuclein Membrane Toxicity by an Unconventional Extracellular Chaperone. *J. Am. Chem. Soc.* **2020**, *142* (21), 9686−9699.
(59) Ahmed, R.; Huang, J.; Akimoto, M.; Shi, T.; Melacini, G. Atomic Resolution Map of Hierarchical Self-Assembly for an Amyloidogenic Protein Probed through Thermal $^{15}N-R_2$ Correlation Matrices. *J. Am. Chem. Soc.* **2021**, *143* (12), 4668−4679.
(60) Beier, A.; Schwarz, T. C.; Kurzbach, D.; Platzer, G.; Tribuzio, F.; Konrat, R. Modulation of Correlated Segment Fluctuations in IDPs upon Complex Formation as an Allosteric Regulatory Mechanism. *J. Mol. Biol.* **2018**, *430* (16), 2439−2452.
(61) Wu, K. P.; Kim, S.; Fela, D. A.; Baum, J. Characterization of conformational and dynamic properties of natively unfolded human and mouse alpha-synuclein ensembles by NMR: Implication for aggregation. *J. Mol. Biol.* **2008**, *378* (5), 1104−1115.
(62) Wu, K. P.; Weinstock, D. S.; Narayanan, C.; Levy, R. M.; Baum, J. Structural Reorganization of α-Synuclein at Low pH Observed by NMR and REMD Simulations. *J. Mol. Biol.* **2009**, *391* (4), 784−796.

https://doi.org/10.1021/jacsau.3c00655
JACS Au 2023, 3, 3485−3493